Digest Journal of Nanomaterials and Biostructures Vol. 17, No. 4, October-December 2022, p. 1453-1461

The determination of urbach energy and optical gap energy by many methods for Zn doped NiO thin films fabricant semiconductor by spray pyrolysis

C. Zaouche[a,*], A. Gahtar[b], S. Benramache[a], Y. Derouiche[c], M. Kharroubi[c], A. Belbel[d], C. Maghni[e], L. Dahbi[f]

[a]*Material Sciences Department, Faculty of Science, University of Biskra, 07000 Biskra, Algeria*

[b]*Department of biology, Faculty of sciences, University Elchahid Hamma Lakhder, 39000 El Oued,Algeria*

[c]*Physico-chemistry of Materials and Environment Laboratory, ZianeAchour University of Djelfa, BP 3117, Djelfa, Algeria*

[d]*ElCherifeBouchouchaAflou University Center, Algeria*

[e]*Department of Physics, Faculty of Science, Med Boudiaf University-M'Sila, Bp 166, 28000 M'sila, Algeria*

[f]*Teacher College of Setif, Algeria*

The effect of Zn doping on optical, structural and electrical properties of $Ni_{1-x}Zn_xO$ thin films has been successfully deposited on glass substrate by Spray Pyrolysis technique. The main objective of this research is to study the $Ni_{1-x}Zn_xO$ thin films to determine the optical gap energy by various methods and compare it with calculated values. The transmission spectra shows that the $Ni_{1-x}Zn_xO$ thin films have a good optical transparency in the visible region. The optical gap energy varied between 3.50 and 3.75 eV, which was determined by various methods and equations. they are explained in the curves of A, A^2, α, α^2 $(Ahυ)^2$ and $(αhυ)^2$ as a function of the photon energy hυ. We observed that the suitable method to calculate the optical gap energy is $(Ahυ)^2$ versus hυ, but this method can't be related to the film thickness. The urbach energy of the $Ni_{1-x}Zn_xO$ thin films also was determined by the curves of LnA and Lnα as a function of photon energy hυ. We deduced that LnA versus hυ is also suitable to estimate the urbach energy. However, the $Ni_{0.90}Zn_{0.10}O$ thin films have a few defects with minimum value of urbach energy. The $Ni_{0.90}Zn_{0.10}O$ thin films have maximum value of optical gap energy. XRD patterns of the $Ni_{1-x}Zn_xO$ thin films indicate that films are polycrystalline with cubic structure. The electrical conductivity of our films is in the order of $9*10^{-3}(\Omega.cm)^{-1}$.

(Received August 15, 2022; Accepted December 12, 2022)

Keywords: Nickel oxide, Thin films, Spray pyrolysis technique, Doping, Optical gap energy, Urbach energy

1. Introduction

Nickel oxide is one of the most important semiconductor materials in the environmental field due to the detecting ability of toxic gases [1]. Nickel oxide (NiO) has a several different applications in the field of pizoelectronic, optoelectronic, environmental and renewable energy such as sensors, fuel cell electrodes, catalysis, thermoelectric devices, dye-sensitized solar cells (DSSCs) and electrochromic material for displays [2–8]. Moreover, it is used to find suitable material with enhanced properties for gas sensing applications for detecting the sensibility in the environment such as NOx, SOx, CO, CO_2…, at high temperature. Because of its semiconductor nature with controlling optical transparency and electrical conductivity, finding the form of the applied interaction is significant. However, several studies have been made to find that the NiO have a high optical transparency and good electrical conductivity at various experimental conditions. NiO thin films have a direct band gap ranging from 3.5 to 4.3 eV [9–10].

* Corresponding author: zaouchechouaieb@gmail.com
https://doi.org/10.15251/DJNB.2022.174.1453

Nickel oxide is used as thin layers, which can be deposited in several methods, including molecular beam epitaxy (MBE), electrochemical deposition, pulsed laser deposition (PLD), chemical vapor deposition and spray Sol–Gel methods, spray pyrolysis technique [11–17]. We used the zinc doped NiO thin films to improve the optical and electrical properties of deposited thin films. This is a metal transition in the periodic table, which was used in the research because of some rare earth material quality due to the increase in the optical band gap energy (broadening).

In this work, we have prepared Zn doped NiO thin films by using the spray pyrolysis technique deposition on glass substrate. Its temperature is 480 C° for 8 minutes. Zn doped NiO thin films were synthesized with different doping levels (0, 0.03, 0.06, 0.10 and 0.13 at.%) for $Ni_{1-x}Zn_xO$. However, we have studied the change of the optical, structural and electrical properties of $Ni_{1-x}Zn_xO$ thin films which fabricate semiconductor with different doping levels x. However, we used the $Ni_{1-x}Zn_xO$ thin films to determine the optical gap energy by various methods for comparing the experimental values.

2. Experimental procedure

$Ni_{1-x}Zn_xO$ solutions were prepared by dissolving the nickel acetate ($Ni(CH_3.CO_2)_2.4H_2O$) and zinc acetate ($Zn(CH_3.CO_2)_2.2H_2O$) with 0.5 mol l^{-1}. In this work, we have used a Zn doping with various concentrations in the game Zn/Ni = 0, 3, 6, 10 and 13 at.% or (x = 0, 0.03, 0.06, 0.10 and 0.13). Then, we have added a drop of HCl to stabilize heating solution. The mixture solution was stirred at room temperature and heated at 40 °C for 2 h to yield a clear and transparent solution. The coating was made 1 day after the precursor was prepared.

The $Ni_{1-x}Zn_xO$ samples were prepared by spraying the coating solution onto glass substrate. Its temperature is 480 °C for 8 minutes to obtain a thin film. The prepared $Ni_{1-x}Zn_xO$ thin films at different Zn doping levels are 0 at.%, 3 at.%, 6 at.%, 10 at.% and 13 at.%. After the deposition of the thin layers, we left substrate to decrease its temperature to the one of the room.

The structural properties of $Ni_{1-x}Zn_xO$ thin films were studied by means of X-ray diffraction (XRD Bruker AXS-8D) with CuKa radiation (λ=0.15406 nm) in the scanning range of (1h) which was between 20° and 70°. The optical transmission of the deposited films was measured in the range of (300–900nm) by using an ultraviolet-visible spectrophotometer (LAMBDA 25) and the electrical conductivity σ was measured by four point methods.

3. Results and discussion

3.1. Structural properties of $Ni_{1-x}Zn_xO$ thin films

The structural characterization of the $Ni_{1-x}Zn_xO$ thin films is carried out by X-ray diffraction method that is shown in figure 1. XRD spectra indicate that the films exhibit polycrystalline structure that belongs to the cubic type of NiO (JCPDS) No. 73-1519) [18]. Figure 1 shows that the XRD peaks at 37.28° and 43.10° corresponding to (111) and (200) crystal planes respectively, the peaks position was accordant with AbdurRahman et al. [19]. We observed that the intensity of (111) and (002) peaks increases in thin films with the increasing doping levels x at x=0.13. This information confirmed that the preferred orientation is along to (111) and (002) planes. However, the film at x=0.13 has higher and sharper diffraction peaks indicating an enhancement of crystallinity with comparison to other films.

The structure information was defined by the diffraction peak angles of the Zn doped NiO thin films (see Table 1). The lattice parameter *a* of Zn doped NiO thin films was calculated from XRD patterns by using the following equation [20]:

$$\frac{1}{d_{hkl}^2} = \frac{h^2 + k^2 + l^2}{a^2} \tag{1}$$

where h, k and l are the Miller indices of the planes. a is the lattice parameter and d_{hkl} is the interplanar spacing. The crystallite sizes G of (111) and (200) planes were calculated according to the Scherer equation [21]:

$$G = \frac{0.9\lambda}{\beta \cos\theta} \quad (2)$$

where G is the crystallite size, $\beta$is the full width at half-maximum (FWHM), $\theta$is Bragg angle of the diffraction peaks and $\lambda$is the X-ray wavelength (λ=0.15406 nm). The variations are shown in Tables 1 and 2.

The variations of the crystallite size and diffraction angle according to (111) and (200) peaks presented in Figure 2 a and b shows the variation of crystallite size and diffraction angle of Zn doped NiO thin films as a function of Zn doping level. In Figure 2a, we have observed that the diffraction angles of (111) plan decreased with increasing doping levels x from 0.06 to 0.13 (see Tables 1). The crystallite size of (111) plan decreased to minimum value obtained at x=0.06 (see Tables 1). On the other hand, Figure 2b shows that the diffraction angles of (200) plan decreased then increased and decreased again with increasing doping levels x to reach the minimum value obtained at x=0.06 (see Table 2). But we observed that the crystallite size of (200) plan decreased to minimum value at x=0.06. The decrease of the crystallite size has been indicated by the enhancement of the crystallinity and a-axis orientation of Zn doped NiO thin films. These phenomena were observed in [22–25]. This result can be explained by coalescence of the crystallite of the thin films to improve oxygen diffusion [26].

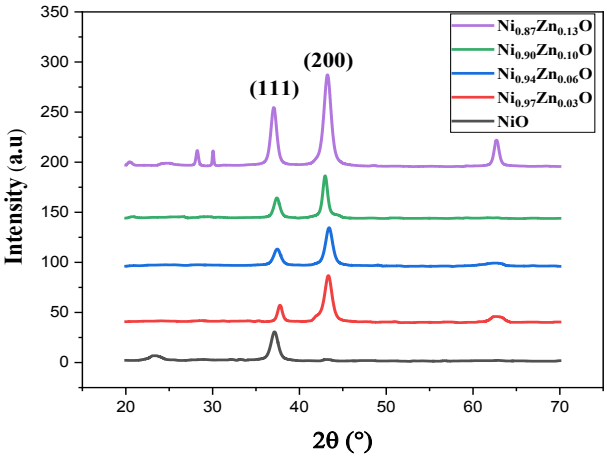

Fig. 1. X-ray diffraction of $Ni_{1-x}Zn_xO$ thin films as a function of Zn doping level.

Table 1. The structural parameters of $Ni_{1-x}Zn_xO$ thin film as a function of Zn doping level of (111) diffraction peak.

x	2θ(°)	d (nm)	$\beta_{1/2}$ (°)	G(nm)	a(nm)
0	37.3381	0,24076	0.3936	21.3143	0,417009
0.03	37.2981	0,241009	0.6298	13.319	0,41744
0.06	37.4183	0,240263	0.9446	8.88342	0,416147
0.10	37.3362	0,240772	0.7872	10.6571	0,41703
0.13	37.0637	0,24248	0.6298	13.3098	0,419987

Table 2. The structural parameters of $Ni_{1-x}Zn_xO$ thin film as a function of Zn doping level of (200) diffraction peak.

x	2θ(°)	d (nm)	$\beta_{1/2}$ (°)	G(nm)	a(nm)
0	42.9067	0,210714	0.3149	27.1177	0,421428
0.03	42.9053	0,21072	0.4723	18.0803	0,421441
0.06	43.3430	0,208693	0.7872	10.8641	0,417386
0.10	42.9439	0,21054	0.6298	13.5606	0,42108
0.13	43.3698	0,20857	0.2362	36.2109	0,417141

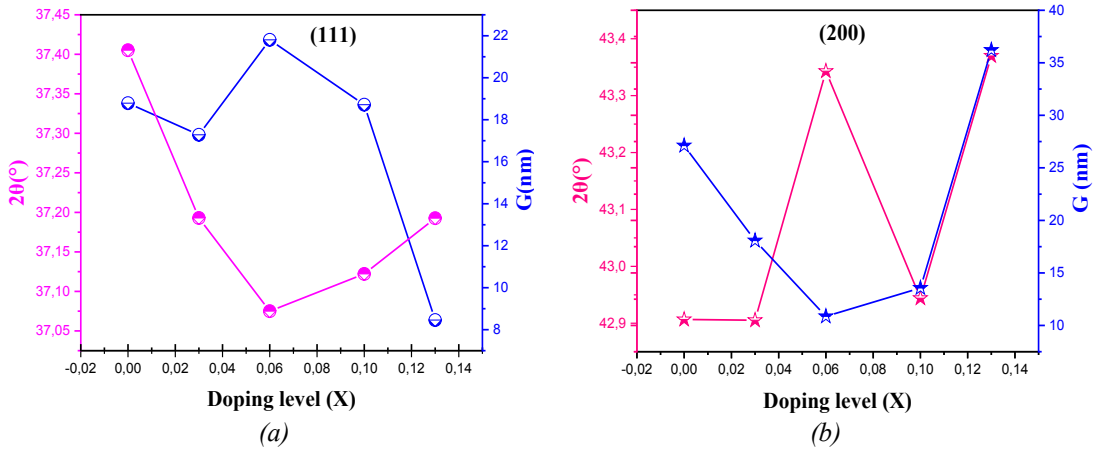

Fig. 2. The variation of crystallite size and diffraction angle of Zn doped NiO thin films according to a (111) phase and b (200).

3.2. Optical properties of $Ni_{1-x}Zn_xO$ thin films

Figure 3 shows the variation of transmittance of $Ni_{1-x}Zn_x$Othin films in the range of 300–900 nm of the wavelength. The prepared $Ni_{1-x}Zn_x$Othin films have an average transmittance at 78–82%. However, the high transparency was obtained in Zn doped NiO thin film with 13 at.% due to the interstitial site of Ni and Zn.

The optical energy gap (E_g) allows the direct transitions between the edge of the valence and conduction band. In this work, we have used six models to determine the optical band gap energy in the NiO thin films which are presented in figure 4. These models were based on the absorbance and absorption coefficient, here the optical energy was determined by the extrapolation of linear curve of A, A^2, α, α^2 $(Ahυ)^2$ and $(\alpha hυ)^2$ as a function of the photon energy hυ. It has been noticed that all the prepared thin films have a different absorption coefficient α in visible range of the spectrum (see figure 4c), the high absorption coefficient value can be explained by the film thickness with increasing of Zn doping. Therefore, we have used these models to compare the calculated optical energy in the $Ni_{1-x}Zn_x$Othin films. Figure 4a–f shows the curves of A, A^2, α, α^2 $(Ahυ)^2$ and $(\alpha hυ)^2$ as a function of the photon energy hυ, respectively. As shown in figure 4a–f, the intersection of the linear region on the hυ axis gives the E_g. It is determined by the transmission spectra according to the following equations [27–29]:

$$A = \alpha d = -\ln T \tag{3}$$

$$(Ahυ)^2 = B\left(h\upsilon - E_g\right) \tag{4}$$

Or

$$(\alpha h\upsilon)^2 = C(h\upsilon - E_g) \tag{5}$$

where A is the absorbance, d is the film thickness, T is the transmission spectra of thin films, α is the absorption coefficient values, B and C is a constant, hυ is the photon energy and E_g is the band gap energy of Zn doped NiO thin films. The films thickness of $Ni_{1-x}Zn_xO$thin films are presented in Table 3.

The variations of calculated optical gap energy of $Ni_{1-x}Zn_xO$thin films are presented in figure 5, which shows the optical gap energy of the $Ni_{1-x}Zn_xO$thin films varied according to the doping level x in the range (3.50–3.75eV) and according to the used methods. It looks like the optical gap energy of the $Ni_{1-x}Zn_xO$thin films decreased when Zn increased from 0 to 6 at.%. The optical gap energy increased when Zn doped level is more than 6 at.%. The optical gap energy has the smallest value when the doping is at 6 at.%. This can be explained by the transition d–d in Ni of Zn. As can be seen that the band gap energy E_g is related to the calculation methods and Zn doping level. It is clear that the calculated optical energy by A and α is less than one which is calculated by other methods. On other hand, we found that the suitable method to calculate the optical energy is $(Ah\upsilon)^2$ function hυ.

The same thing as the optical gap, the urbach energy (E_u) is also related to the disorder in the film network, as it is expressed as follows [30–31]:

$$A = A_0 \exp\left(\frac{h\upsilon}{E_u}\right) \tag{6}$$

$$\alpha = \alpha_0 \exp\left(\frac{h\upsilon}{E_u}\right) \tag{7}$$

where A_0 and α_0 are constants and E_u is the urbach energy. The urbach energy was also determined by the curves of (LnA) and (Lnα) function of photon energy hυ. They are used to deduce the urbach energy of $Ni_{1-x}Zn_xO$thin films as presented in figure 6a and b.

In figure 7, we have found that the variation of the urbach energy in the $Ni_{1-x}Zn_xO$thin films is related to Zn doping level. As clearly seen, the curve of (LnA) function hυ is also suitable to determine the urbach energy of NiO thin films. However, the $Ni_{1-x}Zn_xO$thin films have a few defects with minimum value of urbach energy. It increased then decreased according to the doping level. We obtained the minimum value of urbach energy of the $Ni_{1-x}Zn_xO$thin films at 10 at.% of Zn doping.

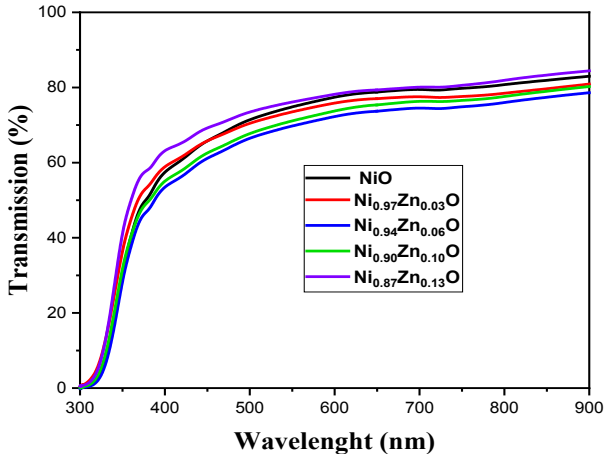

Fig. 3. Transmission spectra of $Ni_{1-x}Zn_xO$ thin films as a function of Zn doping level.

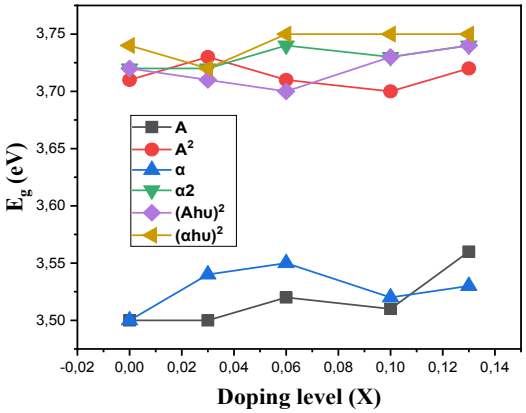

Fig. 5. The variations of optical band gap of $Ni_{1-x}Zn_xO$ thin films as a function of Zn doping level.

Table 3. Variation of film thickness of $Ni_{1-x}Zn_xO$ thin films as a function of Zn doping level.

Zn doping NiO thin films (at.%)	0	3	6	10	13
Film thickness (nm)	334.02	334.08	334.00	334.10	334.13

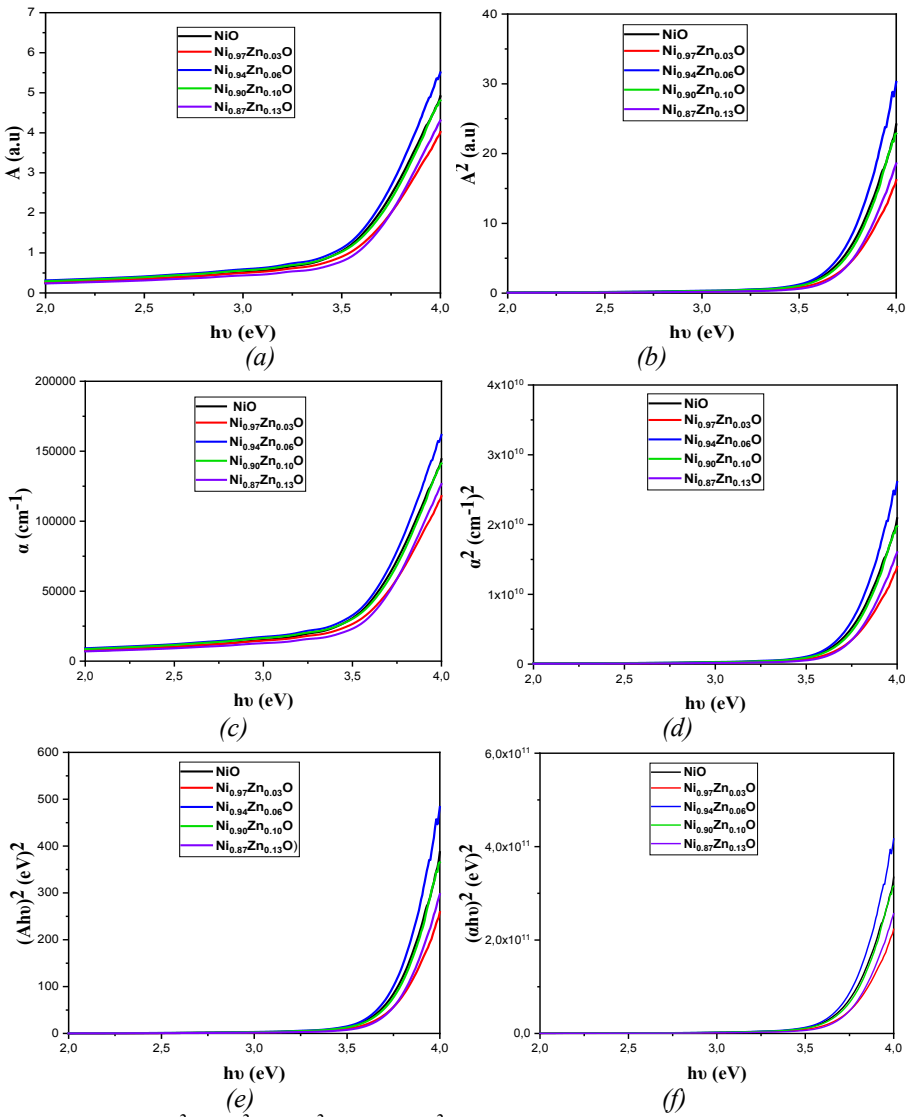

Fig. 4. (a-f) Plot of A, A^2, α, $α^2$ $(Ahυ)^2$ and $(αhυ)^2$ versus (hυ), respectively, in $Ni_{1-x}Zn_xO$ thin films for different Zn doping levels.

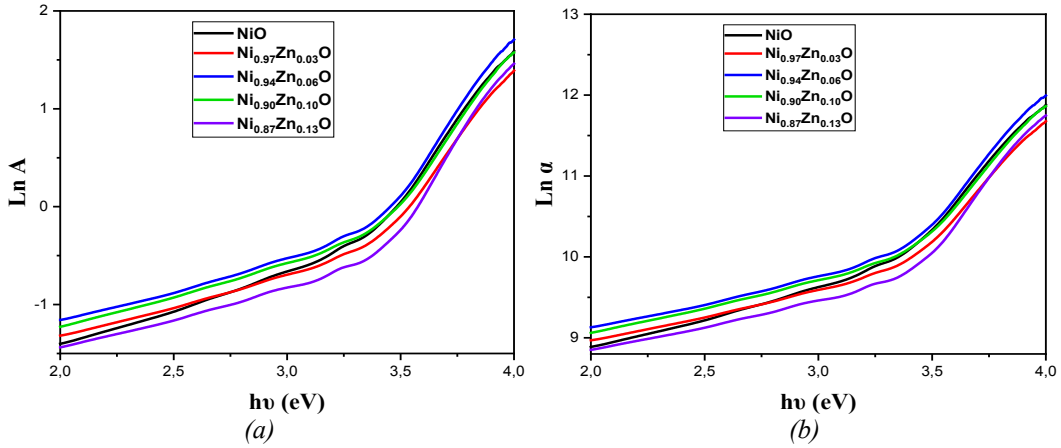

Fig. 6. (a) and (b) The drawn of lnA and lnα as a function of photon energy (hυ), respectively, for deduce the Urbach energy for $Ni_{1-x}Zn_xO$ thin films.

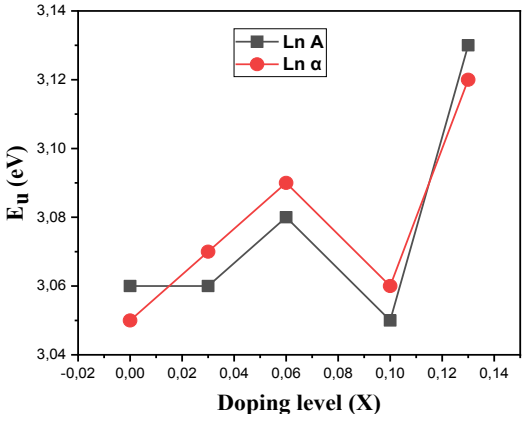

Fig. 7. The variation of Urbach energy of $Ni_{1-x}Zn_xO$ thin films as a function of Zn doping level.

3.3. Electrical properties of $Ni_{1-x}Zn_xO$ thin films

The four-points probe method was used to determine the electrical conductivity of $Ni_{1-x}Zn_xO$ thin films, it is based on measuring the sheet resistance of the films as expressed by:

$$R_{sh} = \frac{\pi}{\ln(2)} . \frac{V}{I} \tag{8}$$

where I is the applied currant = 1 nA and V is the measurement voltage. However, the electrical conductivity σ is also determined by the following equation:

$$\sigma = \frac{1}{d . R_{sh}} \tag{9}$$

Figure 8 shows the variation of the electrical conductivity of Zn doped NiO thin films as a function of Zn doping level. As can be seen, the electrical conductivity increases with increasing the Zn doping level up to 6 at.%. The maximum conductivity value is $0.0135(\Omega.cm)^{-1}$. However, we obtained a small value of the electrical conductivity when Zn doping is 13 at.%. The increase in the conductivity of the $Ni_{1-x}Zn_xO$ thin films can be explained by the displacement of the electrons. The latter comes from the Zn^{+2} donor ions in the substitutional sites of Ni^{+2} and formation of the molecular NiZnO existed on the surface. The decrease in the conductivity of

deposited films after 6 at.% can be related to the increase of the potential barriers, because the introduced atoms are segregated into the grain boundaries [32].

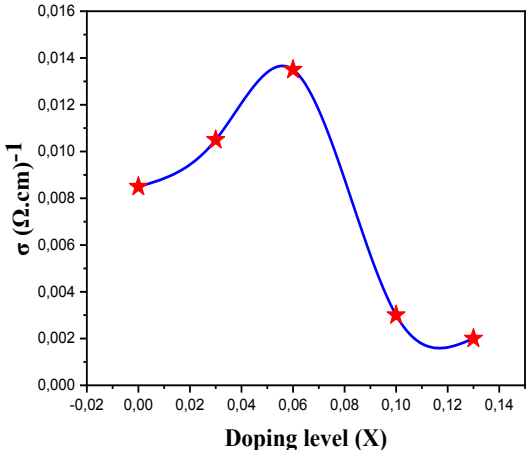

Fig. 8. The electrical conductivity variation of $Ni_{1-x}Zn_xO$ thin films as a function of Zn doping level.

4. Conclusion

In this study, zinc doped Nickel Oxide thin films (Zn/Ni = 0, 3, 6, 10 and 13 at.%) were successfully deposited on glass substrate by Spray Pyrolysis technique using Nickel acetate and Zinc acetate. The transmission spectra of $Ni_{1-x}Zn_xO$ thin films indicated that the $Ni_{1-x}Zn_xO$ thin films become transparent in the visible region. The variation of the optical gap energy was located between 3.50 and 3.75 eV. It was determined by various methods to compare the calculated values.they are explained in the curves of A, A^2, α, α^2 $(Ah\upsilon)^2$ and $(\alpha h\upsilon)^2$ as a function of the photon energy hυ. We observed that the suitable method to calculate the optical energy is $(Ah\upsilon)^2$ function hυ. We observed also that the suitable method to calculate the Urbach energy is LnA function hυ. However, the $Ni_{0.90}Zn_{0.10}O$ thin films have minimum value of urbach energy.The $Ni_{0.90}Zn_{0.10}O$ thin films have maximum value of optical gap energy. XRD patterns of the $Ni_{1-x}Zn_xO$ thin films indicate that films are polycrystalline with cubic structure. The electrical conductivity of deposited films is in the order of $9*10^{-3}(\Omega.cm)^{-1}$.

References

[1] V. Verma, M. Katiyar, Thin Solid Films 527, 369(2013); https://doi.org/10.1016/j.tsf.2012.12.020

[2] S. C. Chen, T. Y. Kuo, Y. C. Lin, H. C. Lin, Thin Solid Films 519(15), 4944(2011) ; https://doi.org/10.1016/j.tsf.2011.01.058

[3] R. Sharma, A. D. Acharya, S. B. Shrivastava, M. M. Patidar, M. Gangrade, T. Shripathi, V. Ganesan, Optik 127(11), 4661(2016) ; https://doi.org/10.1016/j.ijleo.2016.01.050

[4] S. Benramache, M. Aouassa, Journal of Chemistry and Materials Research 5(6), 119(2016).

[5] S. Dendouga, S. Benramache, S. Lakel, Journal of Chemistry and Materials Research 5(4), 78(2016).

[6] D. Dini, Y. Halpin, J. G. Vos, E. A. Gibson, Coordination Chemistry Reviews 304-305, 179(2015) ; https://doi.org/10.1016/j.ccr.2015.03.020

[7] G. F. Cai, C. D. Gu, J. Zhang, P. C. Liu, X. L. Wang, Y. H. You, J. P. Tu, Electrochimica Acta 87, 341(2013) ; https://doi.org/10.1016/j.electacta.2012.09.047

[8] A. C. Nwanya, S. U. I. Offiah, C. Amaechi, S. Agbo, S. C. Ezugwu, B. T. Sone, R. U. Osuji, M. Maaza, F. I. Ezema, Electrochimica Acta 171,128(2015) ;

https://doi.org/10.1016/j.electacta.2015.05.005
[9] R. Romero, F. Martin, J. R. Ramos-Barrado, D. Leinen, Thin Solid Films 518(16), 4499(2010) ; https://doi.org/10.1016/j.tsf.2009.12.016
[10] T. Chtouki, L. Soumahoro, B. Kulyk, H. Bougharraf, B. Kabouchi, H. Erguig, B. Sahraoui, Optik 128, 8(2017) ; https://doi.org/10.1016/j.ijleo.2016.10.007
[11] R. J. Deokate, R. S. Kalubarme, C. J. Park, C. D. Lokhande 224, 378(2017) ; https://doi.org/10.1016/j.electacta.2016.12.034
[12] Y. Yu, X. Li, Z. Shen, X. Zhang, P. Liu, Y. Gao, T. Jiang, J. Hua, Journal of Colloid and Interface Science 490, 380(2017) ; https://doi.org/10.1016/j.jcis.2016.11.037
[13] S. U. Offiah, M. O. Nwodo, A. C. Nwanya, S. C. Ezugwu, S. N. Agbo, P. U. Ugwuoke, R. U. Osuji, M. Malik, F. I. Ezema, Optik 125, 2905(2014); https://doi.org/10.1016/j.ijleo.2013.11.073
[14] S. C. Chen, T. Y. Kuo, Y. C. Lin, S. W. Hsu, H. C. Lin, Thin Solid Films 549, 50(2013) ; https://doi.org/10.1016/j.tsf.2013.07.017
[15] X. H. Xia, J. P. Tu, J. Zhang, X. L. Wang, W. K. Zhang, H. Huang, Electrochimica Acta 53(18), 5721(2008) ; https://doi.org/10.1016/j.electacta.2008.03.047
[16] I. Castro-Hurtado, J. Herra'n, G. G. Mandayo, E. Castan˜o, Thin Solid Films 520(3), 947(2011) ; https://doi.org/10.1016/j.tsf.2011.04.180
[17] C. Zaouche, Y. Aoun, S. Benramache, A. Gahtar, Scientific Bulletin of valahia University materials and mechanics 17(17), 27(2019); https://doi.org/10.2478/bsmm-2019-0015
[18] J. Cao, Z. Wang, R. Wang, S. Liu, T. Fei, L. Wanga, T. Zhang, Materials Chemistry A 3(10), 5635(2015) ; https://doi.org/10.1039/C4TA06892K
[19] M. AbdurRahman, R. Radhakrishnan, R. Gopalakrishnan, Alloys and Compounds 742, 421(2018) ; https://doi.org/10.1016/j.jallcom.2018.01.298
[20] A.F. Saleh, Application or Innovation in Engineering & Management 2(1), 16 (2013).
[21] A. Gahtar, S. Benramache, A. Ammari, A. Boukhachem, A. Ziouche, Inorganic and Nano-Metal Chemistry 52(1), 112(2022) ; https://doi.org/10.1080/24701556.2020.1862225
[22] N. Beji, M. Reghima, M. Souli, N.K. Turki, Alloys and Compounds 675, 231 (2016) ; https://doi.org/10.1016/j.jallcom.2016.03.115
[23] S. Chatterjee, S.K. Saha, A.J. Pal, Solar Energy Materials and Solar 147, 17 (2016) ; https://doi.org/10.1016/j.solmat.2015.11.045
[24] F.J. Garcia-Garcia, P. Salazar, F. Yubero, A.R. González-Elipe, Electrochimica Acta 201, 38 (2016) ; https://doi.org/10.1016/j.electacta.2016.03.193
[25] N. Ali, A. Hussain, R. Ahmed, M.K. Wang, C. Zhao, B. UlHaq, Y.Q. Fu, Renewable and Sustainable Energy Reviews 59, 726 (2016); https://doi.org/10.1016/j.rser.2015.12.268
[26] S. Benramache, B. Benhaoua, Superlattices and Microstructures 52(16), 1062 (2012) ; https://doi.org/10.1016/j.spmi.2012.08.006
[27] R. Dridi, M. BenAmor, N. Mahdhi, A. Amlouk, K. Boubaker, M. Amlouk, Journal of Non-Crystalline Solids 449, 1(2016) ; https://doi.org/10.1016/j.jnoncrysol.2016.07.008
[28] A. A. Al-Ghamdi, M. Sh. Abdel-wahab, A. A. Farghali, P. M. Z. Hasan, Materials Research Bulletin 75, 71(2016) ; https://doi.org/10.1016/j.materresbull.2015.11.027
[29] Gahtar, A., Benali, A., Benramache, S., &Zaouche, C, Chalcogenide Letters, 19(2), 1(2022) ; https://doi.org/10.15251/CL.2022.192.103
[30] N. S Kumar, K. V. Bangera, C. Ananda, G. K. Shivakumar, Journal of Alloys and Compounds 578, 613(2013) ; https://doi.org/10.1016/j.jallcom.2013.07.036
[31] S. Benramache, B. Benhaoua, Superlattices and Microstructures 52(6), 1062(2012) ; https://doi.org/10.1016/j.spmi.2012.08.006
[32] S. Benramache, B. Benhaoua, F. Chabane, Journal of Semiconductors 33(9), 093001(2012) ; https://doi.org/10.1088/1674-4926/33/9/093001